Supporting Information

1,2-H versus 1,2-C-shift on Sn-Silsesquioxanes

Tyler R. Josephson[1], Stephen K. Brand[2], Stavros Caratzoulas[3*], Dionisios G. Vlachos[1,3]

[1]*Department of Chemical and Biomolecular Engineering, University of Delaware, Newark, DE 19716*

[2]*Division of Chemistry and Chemical Engineering, California Institute of Technology, Pasadena, CA 91125*

[3]*Catalysis Center for Energy Innovation, University of Delaware, Newark, DE 19716*

[*]*Corresponding author: cstavros@udel.edu*

Lewis structures from NBO analysis of catalysts 1a and 1b

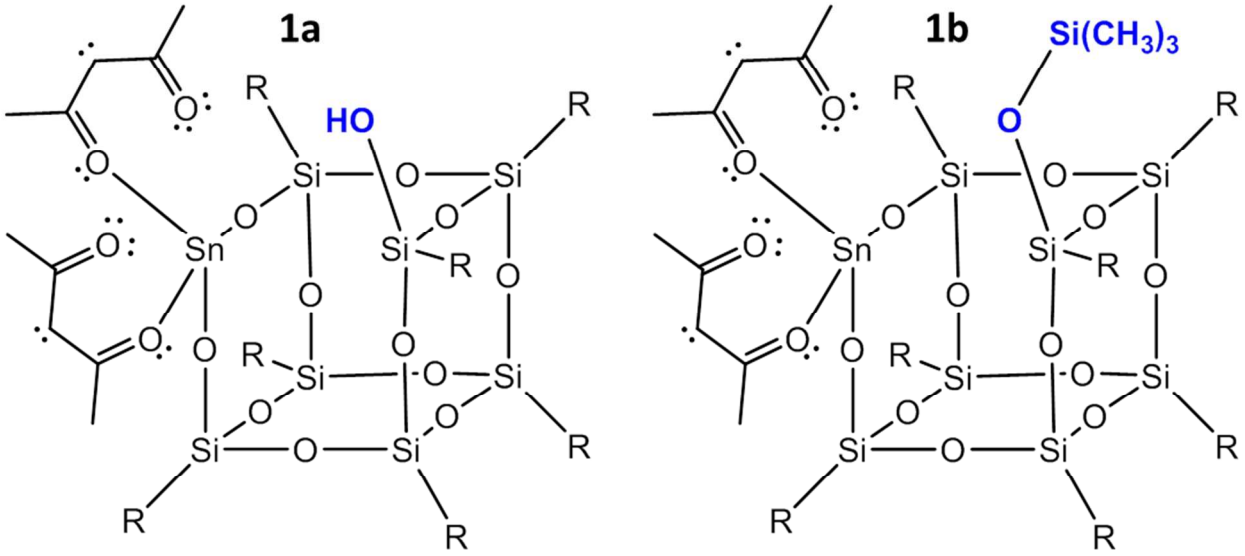

Figure S1. The most stable resonance structures of 1a and 1b are characterized by four covalent Sn-O bonds. Each acac ligand has one bond to Sn, two C=O, a lone pair on C3, and only one lone pair on the O bonded to Sn.

Table S1. Free energies at 353 K for H-shift and C-shift reactions on Sn-O-Si bridges on **1a** and **1b**. Electronic energies were calculated using basis set B (see computational methods), and zero-point corrections and entropic contributions were calculated using basis set A. Free energies are reported with respect to isolated glyceraldehyde and catalyst.

Sn-O-Si Bridge Mechanisms		B-1	B-2 TS	B-3	B-4 TS	B-5	B-6 TS	B-7
1a	H-shift	12.48	24.47	5.57	28.30	11.18	21.55	17.99
	C-shift	12.48	24.47	5.57	32.83	9.73	26.86	22.96
1b	H-shift	2.89	25.61	2.81	27.52	-1.41	8.59	6.16
	C-shift	2.89	25.61	2.81	38.13	1.42	16.26	0.32

		O1-1	O1-2 TS	O1-3	O1-4 TS	O1-5
1a	H-shift	19.40	46.27	7.90	21.82	3.13
	C-shift	20.45	41.19	16.93	26.86	22.96
1b	H-shift	8.45	34.79	0.27	8.59	6.16
	C-shift	13.42	28.27	13.50	20.93	9.47

		O2-1	O2-2 TS	O2-3	O2-4 TS	O2-5
1a	H-shift	13.64	19.06	5.25	37.15	-0.55
	C-shift	13.64	19.06	7.90	42.70	20.75
1b	H-shift	9.61	13.86	0.59	35.27	9.38
	C-shift	9.61	13.86	0.76	37.58	1.82

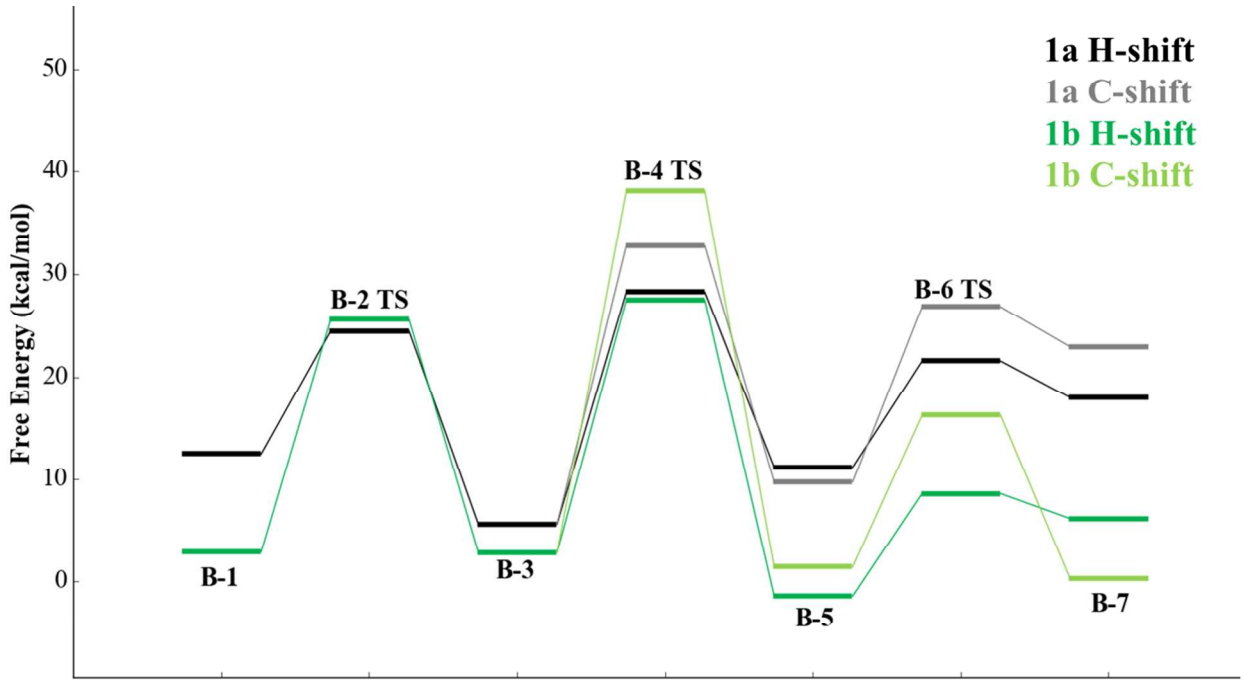

Figure S2 – Free energy profiles of H/C-shift on 1a and 1b through the bidentate pathway.

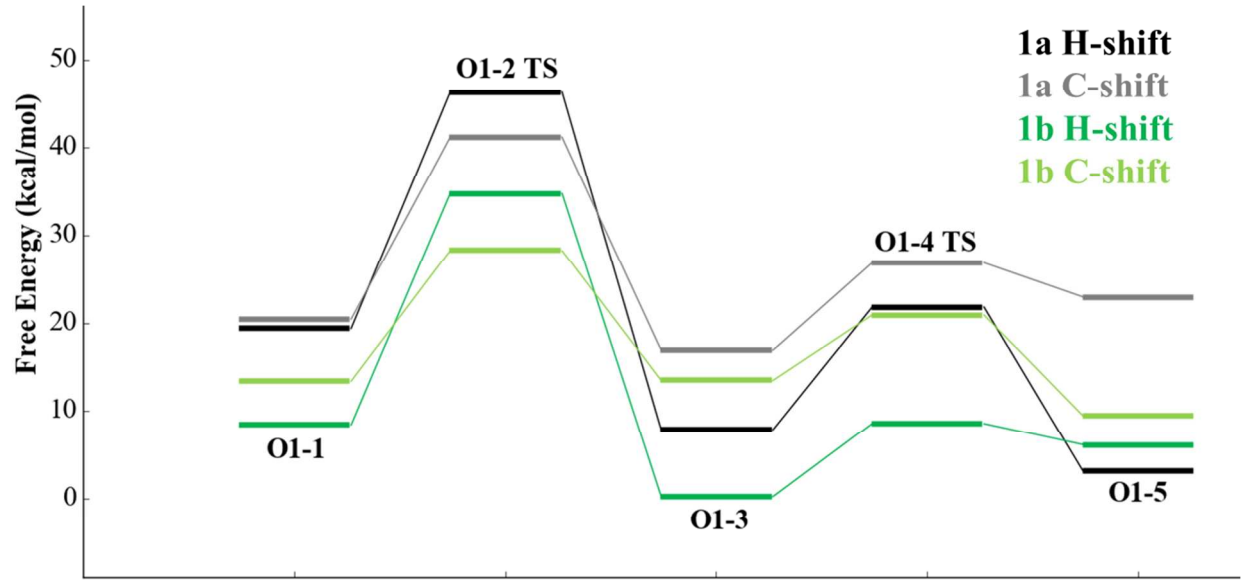

Figure S3 – Free energy profiles of H/C-shift on 1a and 1b through the O1 binding pathway.

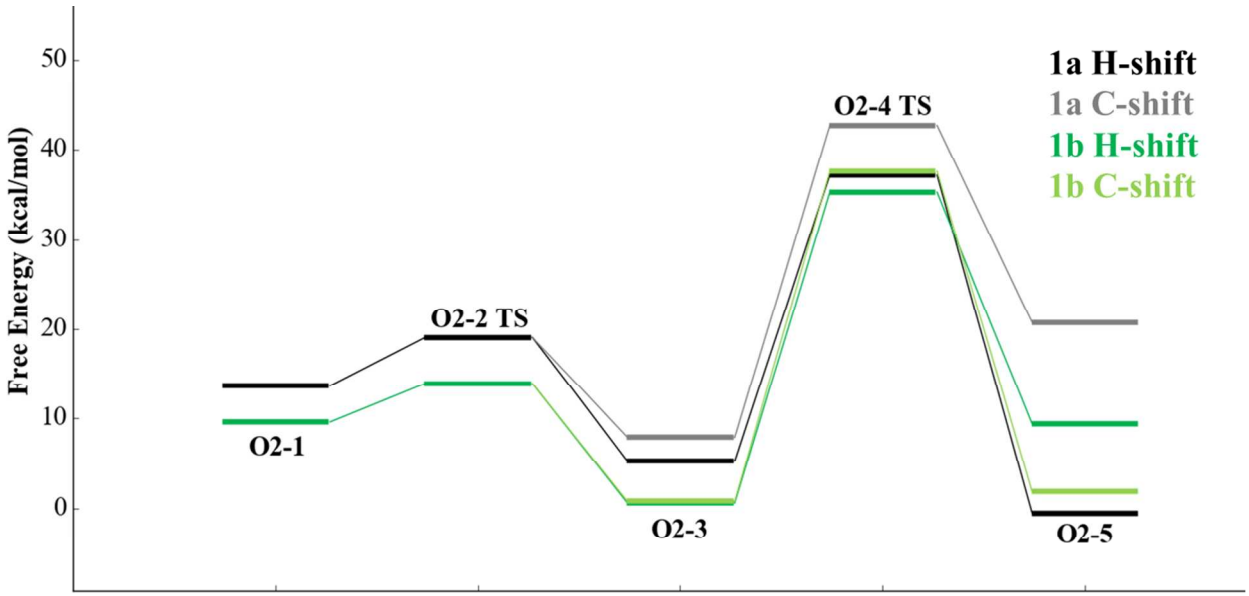

Figure S4 – Free energy profiles of H/C-shift on 1a and 1b through the O2 binding pathway.

Table S2. Free energies at 353 K for H-shift and C-shift reactions using the SiOH moiety in **1a**. Electronic energies were calculated using basis set B (see computational methods), and zero-point corrections and entropic contributions were calculated using basis set A. "sb" indicates a pathway in which the silanol transfers protons to a Sn-O-Si bridge, "la" indicates an acac ligand interacting with O3 of the sugar, "lb" indicates an acac ligand assisting the H-shift through an interaction with the transferring H, and "sl" indicates a proton transfer between the silanol and a ligand O. Free energies are reported with respect to isolated glyceraldehyde and catalyst.

Mechanisms Unique to 1a		O1sb-1	O1sb-2 TS	O1sb-3	O1sb-4 TS	O1sb-5
1a	H-shift	23.00	47.20	11.85	21.55	17.99
	C-shift	14.36	47.59	18.34	18.24	10.43

		O2sb-1	O2sb-2 TS	O2sb-3	O2sb-4 TS	O2sb-5
1a	H-shift	10.43	18.24	20.40	43.20	18.61
	C-shift	10.43	18.24	18.34	47.59	14.36

		O1sb-la-1	O1sb-la-2 TS	O1sb-la-3		
1a	H-shift	16.74	38.77	13.20		

		O1sb-lb-1	O1sb-lb-2 TS	O1sb-lb-3		
1a	H-shift	16.32	32.72	16.72		

		O2sl-1	O2sl-2 TS	O2sl-3	O2sl-4 TS	O2sl-5
1a	H-shift	13.80		12.74	35.09	13.97
	C-shift	13.80		13.80	28.15	18.98

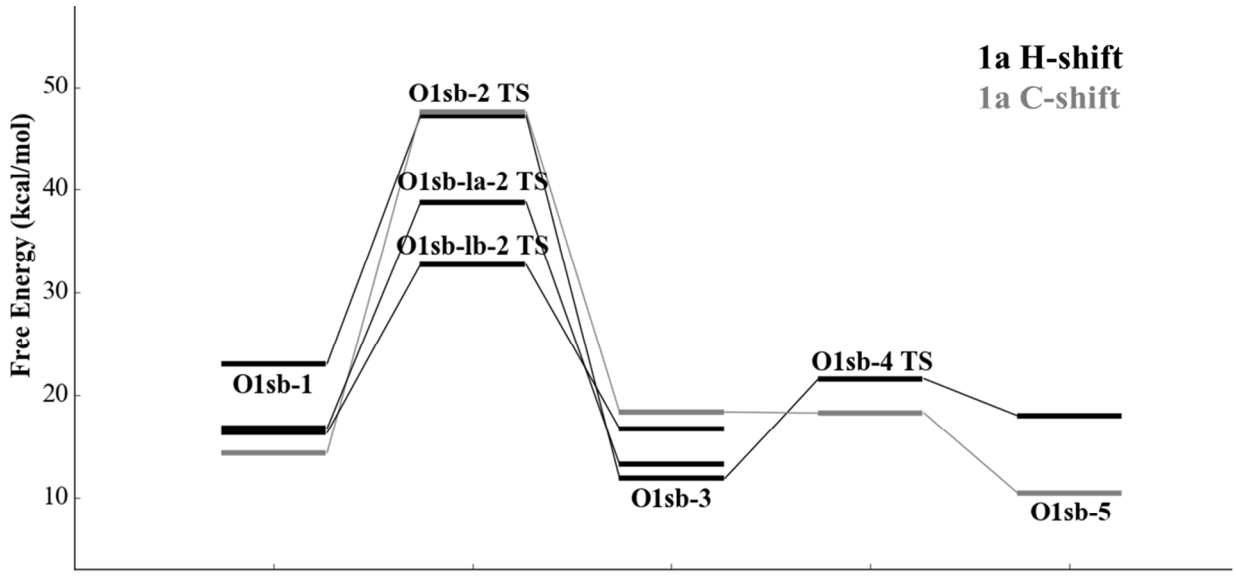

Figure S5 – Free energy profiles of H/C-shift on 1a through the O1sb, O1sb-la, and O1sb-lb pathways.

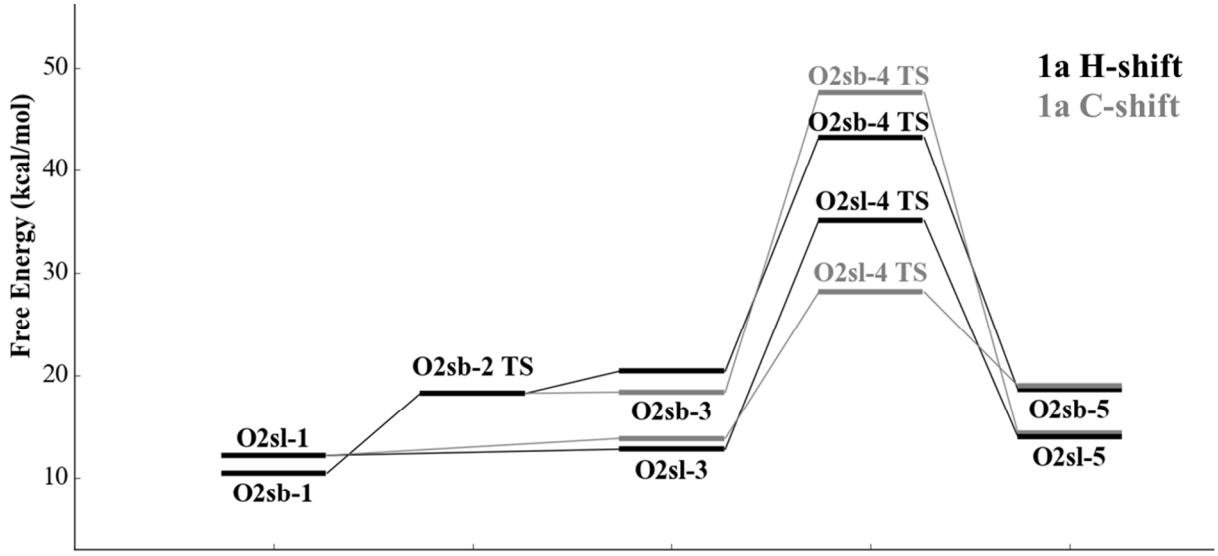

Figure S6 – Free energy profiles of H/C-shift on 1a through the O2sb and O2sl pathways.

Bader Analysis of H/C-shift Transition States on 1a

During the bidentate H-shift reaction, the C2-H bond is stretched from 1.10 to 1.36 Å at the TS. The electron density ρ at the BCP decreases from 0.168 to 0.121, indicating a weakening of the bond, and the Laplacian $\nabla^2(\rho)$ changes sign, from -0.139 to 0.102, indicating a switch from a region of local charge concentration to charge depletion. The ellipticity of the C2-H BCP increases from 3.12e-4 to 3.74, further indicating a dramatic weakening of the bond. At the H-shift TS, the transferring H does not yet have a bond with C1, even though the C1-H distance is only 1.38 Å; no C1-H BCP is observed, nor is there a (3,+1) ring critical point (RCP) present in the C1-C2-H triangle.

Likewise, in the bidentate C-shift reaction, the C2-C3 bond is stretched from the reactant to the C-shift TS, which is accompanied by a decrease in ρ (from 0.173 to 0.078), an increase in $\nabla^2(\rho)$ (from 0.072 to 0.161), and an increase in ellipticity (from 3.90e-3 to 1.06), indicating severe weakening in the C-C bond. The BCP is between C1 and C3 at the TS, but there is no BCP between C2 and C3, nor a RCP in the C1-C2-C3 triangle. The C3-O3 distance contracts slightly, from 1.41 to 1.36 Å, and this is accompanied by an increase in ρ at the BCP from 0.237 to 0.258, a sign change in $\nabla^2(\rho)$ from 0.092 to -0.026, and an increase in ellipticity from 4.89e-3 to 1.70e-2, all signatures of increased π character in the C3-O3 bond. While the C3-O3 bond is strengthened, the O3-H bond is weakened slightly, with a small decrease in ρ from 0.241 to 0.238, a small increase in $\nabla^2(\rho)$ from -0.528 to -0.484, and a slight increase in ellipticity from 4.88e-3 to 6.20e-3.

The bidentate C-shift reaction has a TS energy of 32.8 kcal/mol, the O2sl pathway has a TS energy of 28.2 kcal/mol, and the O1sb pathway has a TS energy of 47.6 kcal/mol. The stability of each TS is correlated to the ρ, $\nabla^2(\rho)$, and ε of the C3-O3 bond, reinforcing the importance of stabilizing the C3 moiety at the C-shift transition state.

Table S3. Bader Analysis of Select Bond Critical Points (BCPs) for gas-phase glyceraldehyde (GLY) and various intermediate and transition states.

Gas-phase GLY	**ρ**	**$\nabla^2(\rho)$**	**ε (ellipticity)**
C2-C3	1.74E-01	6.79E-02	2.33E-03
C2-H	1.68E-01	-1.39E-01	2.08E-03
C3-O3	2.38E-01	8.77E-02	9.09E-03
O3-H	2.42E-01	-5.41E-01	5.56E-03
HO3-O1	2.57E-02	7.34E-02	6.57E-01

OH_H_B-4 DP GLY	**ρ**	**$\nabla^2(\rho)$**	**ε (ellipticity)**
C2-C3	1.73E-01	7.02E-02	3.90E-03
C2-H	1.68E-01	-1.39E-01	3.19E-04

C3-O3	2.37E-01	9.24E-02	4.89E-03
O3-H	2.41E-01	-5.28E-01	4.88E-03
HO3-OHSi	3.46E-02	9.04E-02	1.68E-01

OH_H_B-5 Bidentate H-Shift TS	**ρ**	**$\nabla^2(\rho)$**	**ε (ellipticity)**
C2-C3	1.80E-01	4.84E-02	1.28E-02
C2-H	1.21E-01	1.02E-01	3.47E+00
C3-O3	2.41E-01	7.41E-02	8.45E-03
O3-H	2.38E-01	-4.94E-01	5.52E-03
HO3-OHSi	3.56E-02	9.27E-02	6.78E-03

OH_C_B-5 Bidentate C-shift TS	**ρ**	**∇2(ρ)**	**ε (ellipticity)**
C1-C3	7.83E-02	1.61E-01	1.06E+00
C2-H	1.71E-01	-1.62E-01	7.63E-03
C3-O3	2.58E-01	-2.59E-02	1.70E-02
O3-H	2.38E-01	-4.84E-01	6.20E-03
HO3-OHSi	3.40E-02	8.88E-02	3.61E-02

OH_C_O2sl-4 Ligand-Assist C-Shift TS	**ρ**	**∇2(ρ)**	**ε (ellipticity)**
C2-C3	8.00E-02	1.63E-01	7.94E-01
C2-H	1.71E-01	-1.56E-01	1.06E-02
C3-O3	2.68E-01	-7.71E-02	1.42E-02
O3-H	2.35E-01	-4.54E-01	5.54E-03
HO3-ligand O1	2.97E-02	8.22E-02	6.97E-02
HO3-ligand O2	2.80E-02	7.62E-02	6.81E-02

OH_C_O1sb-2 O1 C-shift TS	**ρ**	**∇2(ρ)**	**ε (ellipticity)**
C1-C2	2.15E-01	-7.01E-02	7.47E-03
C1-C3	8.98E-02	1.67E-01	3.44E-01
C2-H	1.71E-01	-1.58E-01	8.51E-03
C3-O3	2.56E-01	-1.48E-02	1.59E-02
O3-H	2.37E-01	-4.77E-01	5.11E-03
HO3-OLigand	3.58E-02	9.45E-02	9.13E-03